7456 *Macromolecules* **2009**, *42*, 7456–7464
DOI: 10.1021/ma901701w

Macromolecules
ARTICLE

Polymersome Formation from AB_2 Type 3-Miktoarm Star Copolymers

Haiqing Yin, Sun-Woong Kang, and You Han Bae*

Department of Pharmaceutics & Pharmaceutical Chemistry, University of Utah, 421 Wakara Way Suite 315, Salt Lake City, Utah 84108

Received May 27, 2009; Revised Manuscript Received August 28, 2009

ABSTRACT: A series of AB_2 type 3-miktoarm star copolymers that mimic the natural structure of phospolipids were synthesized using poly(ethylene glycol) (PEG) as the A arm and poly(L-lactic acid) (PLLA) as the two B arms. Their ability to self-assemble into polymer vesicles (polymersomes) in aqueous solutions was investigated using a variety of experimental techniques including optical microscopy, confocal laser scanning microscopy, dynamic/static light scattering, transmission electron microscopy, and fluorimetry. Polymersome formation was observed for all the 3-miktoarm polymers tested in a much broader range of the PEG volume fractions (0.2−0.7) than their linear diblock counterparts (0.2−0.4). Furthermore, the water-soluble anticancer drug doxorubicin hydrochloride was successfully encapsulated into the fabricated nano-sized polymersomes, and sustained *in vitro* release of the loaded drug was observed. Finally, possible mechanisms for the superior vesicle-forming capability of the 3-miktoarm architecture were discussed based on both the geometric and thermodynamic viewpoints.

Introduction

Vesicles prepared from natural or synthetic lipids in aqueous solutions (so-called "liposomes") have been studied extensively as drug carriers due to their ability to incorporate both hydrophilic and hydrophobic substances in the water-filled lumen and the membrane wall, respectively. It is recognized that pure liposomes suffer from a very fast blood clearance *in vivo* by the reticuloendothelial system (RES) unless a surface modification approach is applied, usually by coupling a biocompatible polymer chain of poly(ethylene glycol) (PEG) to a small fraction of the lipids to increase the circulation half-life.[1,2] As a result of the low molecular weight of lipids (MW < 1 kDa), many lipid vesicle properties such as encapsulant retention and membrane stability are often not well controlled.[3]

In the past decade, a polymer approach to vesicle formation has emerged to extend the chemical and physical limits of liposomes.[4−7] Vesicles formed in this case, also referred to as "polymersomes", have attracted great interest because of their intriguing aggregation tendencies, cell and virus-mimicking functions, and their tremendous potential for applications in medicine, pharmacy, and biotechnology. Unlike liposomes, the membrane thickness of polymersomes can be readily tailored by adjusting the molecular weight of the hydrophobic moiety of the polymer, and thus a lot of polymersome properties such as elasticity, permeability, and mechanical stability can be finely controlled.[8] Because of the higher molecular weight of polymers as compared to lipids, the membrane of polymersomes is generally thicker, stronger, and tougher and thus inherently more stable than conventional liposomes.[5]

So far, much attention has been focused on polymersomes fabricated in aqueous solutions from a variety of amphiphilic diblock copolymers which are essentially combinations of a hydrophilic moiety and another hydrophobic moiety.[9−11] PEG is a common choice for the hydrophilic block due to its biocompatibility and resistance to both protein adsorption and cellular adhesion, resulting in a prolonged circulation time *in vivo*. Various biodegradable or non-biodegradable polymers have been selected and tested as the hydrophobic block, including but not limited to poly(ε-caprolactone) (PCL),[12] poly(lactic acid) (PLA),[13] polyethylethylene (PEE),[5] polybutadiene (PBD),[14,15] poly(propylene sulfide) (PPS),[16] and poly(2-vinylpyridine).[17] Although some systems have shown potential as long-circulating drug carriers,[18−21] a significant design limitation is that polymersomes can only be formed within a narrow range of hydrophilic volume fractions (0.2−0.4),[22−24] and this confinement may also lead to the coexistence of nonvesicular morphologies for diblock copolymers even with relatively narrow polydispersities.[25] This has motivated the exploration of new polymer scaffolds having better vesicle-forming capabilities.

Inspired by the natural one-head, two-tail molecular structure of phospholipids, we investigated an amphiphilic AB_2 type 3-miktoarm polymer architecture which contains one hydrophilic block and two hydrophobic blocks connected to one central core (Scheme 1a) and tested its ability to form vesicles in aqueous solutions. A series of 3-miktoarm star copolymers with the hydrophilic block volume fractions (f) ranging from 0.2 to 0.7 were synthesized using poly(ethylene glycol) (PEG) (M_n: 2K, 5K Da) as the hydrophilic A arm and biodegradable poly(L-lactic acid) (PLLA) (M_n: 1K−4K Da) as the two hydrophobic B arms (Scheme 1b) as PEG and PLA are among the few polymers that are FDA-approved for good biocompatibility. For comparison, a series of PEG-*b*-PLLA class linear diblock counterparts were also synthesized. It was found that spherical polymersomes can be fabricated by a variety of methods using the 3-miktoarm polymers in a significantly broader range of f values compared to their diblock counterparts, suggesting the 3-miktoarm polymers have superior vesicle-forming abilities. The water-soluble anticancer drug doxorubicin hydrochloride (DOX·HCl) was successfully encapsulated into the nano-sized polymersomes via a remote loading method. The loaded drug showed significant sustained release patterns compared to free drug over a period of 48 h *in vitro*. In the Discussion section, possible mechanisms for the enhanced vesicle-forming ability of the 3-miktoarm architecture were proposed.

*To whom correspondence should be addressed: E-mail you.bae@utah.edu; Fax +1-801-585-3614; Tel +1-801-585-1518.

 Published on Web 09/21/2009

Scheme 1. (a) Structural Analogy between a Phospholipid Molecule (Left) and an AB_2 3-Miktoarm Copolymer (Right) To Form a Bilayer Vesicle; (b) Chemical Structure of PEG_m-*b*-$(PLLA_n)_2$

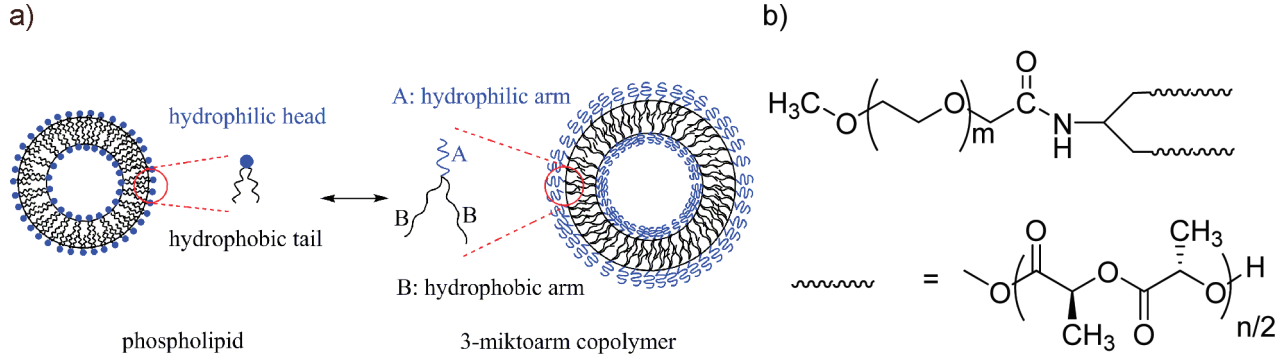

Scheme 2. Synthesis Route for the AB_2 3-Miktoarm Polymer

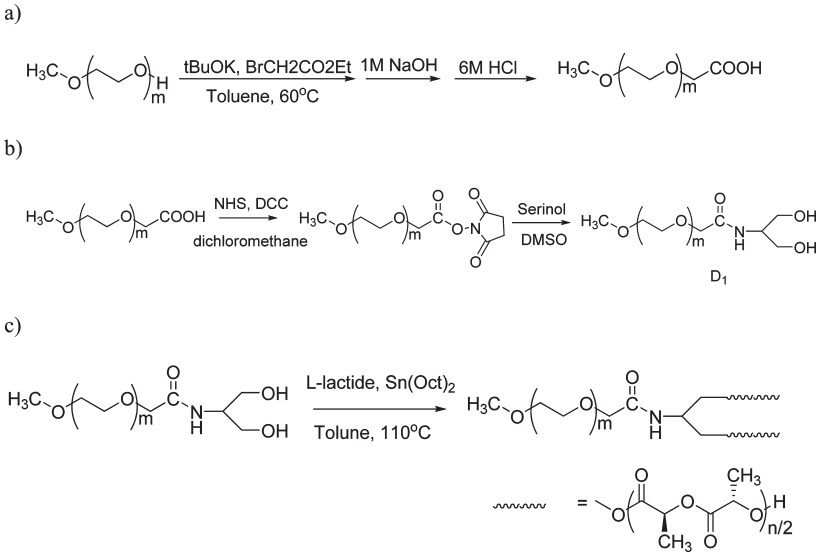

Experimental Section

Materials. L-Lactide, poly(ethylene glycol) methyl ether (PEG, M_n: 2000, 5000 Da), potassium *tert*-butoxide (^{t}BuOK), ethyl bromoacetate ($BrCH_2CO_2Et$), DEAE-Sephadex A-25, *N*-hydroxysuccinimide (NHS), *N*,*N*′-dicyclohexylcarbodiimide (DCC), serinol, stannous octoate ($SnOct_2$), anhydrous toluene, dimethylformamide (DMF), and dimethyl sulfoxide (DMSO) were purchased from Sigma-Aldrich Co. and used as received. FITC-Dextran ($M_n \sim 4000$ Da), Nile red, and doxorubicin hydrochloride (DOX·HCl) were purchased from Sigma and used without further purification. All the other chemicals were at least ACS grade.

Polymer Synthesis. *1. Preparation of Carboxyl-Terminated PEG* (*Scheme 2a*). 10 mmol of poly(ethylene oxide) methyl ether (PEG 2K, 5K Da) was dissolved in 100 mL of toluene at 60 °C, and 40 mmol of ^{t}BuOK was added. After 6 h of reaction, 60 mmol of $BrCH_2CO_2Et$ was added to the solution. The reaction mixture was vigorously stirred at room temperature for 24 h and then filtered; the filtrate was precipitated in cold diethyl ether and dried in vacuo. The obtained product was dissolved in 40 mL of 1 M NaOH with 10 g of NaCl added, and the solution was stirred at room temperature for 2 h and then acidified to pH 3 by the addition of 6 M HCl. The solution was extracted with 40 mL of dichloromethane, dried with anhydrous $MgSO_4$, and then precipitated in diethyl ether. Unreacted PEG was removed by ion-exchange fractionation using a column containing DEAE-Sephadex A-25 tetraborate form to give pure carboxyl-terminated PEG. ^{1}H NMR (400 MHz, $CDCl_3$): δ (ppm) = 3.38 (CH_3−O−CH_2−), 3.65 (−O−CH_2−CH_2−O−), 4.14 (−O−CH_2−COOH).

2. Preparation of Hydroxyl-Terminated Dendron (*Scheme 2b*). 6 mmol of NHS was added to a solution of 4 mmol of carboxyl-terminated PEG in 20 mL of dichloromethane under vigorous stirring, and 5 mmol of DCC was subsequently added as an activator. The reaction mixture was stirred for 24 h at room temperature, allowing DCC to become *N*,*N*′-dicyclohexylurea which was filtered by precipitation at 4 °C. The filtrate was precipitated in cold diethyl ether and dried in vacuo to give PEG-NHS. ^{1}H NMR ($CDCl_3$) δ (ppm) = 2.85 (−N−CO−CH_2−CH_2−CO−), 3.38 (CH_3−O−CH_2−), 3.65 (−O−CH_2−CH_2−O−), 4.52 (−O−CH_2−CO−N−). Hydroxyl-terminated dendron was then obtained by coupling 1 mmol of activated PEG-NHS with excess serinol (7 mmol) in 20 mL of DMSO. The reaction mixture was thoroughly dialyzed against Mili-Q water using a semipermeable membrane (Spectra/Por, MWCO: 2000 Da) to remove unreacted serinol, subsequently extracted with 40 mL of dichloromethane, and precipitated in cold diethyl ether. This precipitate was recrystallized twice to obtain purified hydroxyl-terminated dendron (D_1). ^{1}H NMR ($CDCl_3$) δ (ppm) = 3.38 (CH_3−O−CH_2−), 3.45−3.48 (CH_3−O−CH_2−CH_2−), 3.65 (−O−CH_2−CH_2−O−), 3.76−3.83 (−NH−CH−(CH_2−OH)$_2$), 4.03 (−O−CH_2−CO−NH−), 7.58 (−CO−NH−CH−). A representative ^{1}H NMR plot for PEG_{45} based dendron is shown in Figure S1.

3. Preparation of PEG-Based AB_2 Type 3-Miktoarm Polymers (*Scheme 2c*). The poly(L-lactic acid)-terminated 3-miktoarm polymers were synthesized from controlled ring-opening polymerization of L-lactide monomer using the above hydroxyl-terminated dendron (D_1) as initiator and $SnOct_2$ as catalyst. A

typical reaction example: 500 mg of D_l was first dissolved in 50 mL of toluene in a round-bottomed flask equipped with a Dean−Stark trap, followed by 1 h of azeotropic distillation at 120 °C in a nitrogen atmosphere. After the solution was cooled down to 70 °C, 500 mg of L-lactide and $SnOct_2$ (1 wt % of L-lactide) were added, and the polymerization was carried out at 110 °C in a nitrogen atmosphere for 24 h. The reaction was stopped by the addition of cold diethyl ether, and the precipitate was purified by recrystallization twice in dichloromethane−diethyl ether. ^{1}H NMR ($CDCl_3$) δ (ppm) = 1.58 (−CO−CH(CH_3)−O−), 3.38 (CH_3−O−CH_2−), 3.45−3.48 (CH_3−O−CH_2−CH_2−), 3.65 (−O−CH_2−CH_2−O−), 3.76−3.83 (−NH−CH−(CH_2−OH)$_2$), 4.03 (−O−CH_2−CO−NH−), 5.14−5.23 (−CO−CH(CH_3)−O−), 7.05 (−CO−NH−CH−). Figure S2 shows the NMR plot of PEG$_{45}$-*b*-(PLLA$_{32.5}$)$_2$.

4. Preparation of PEG-b-PLLA Diblock Polymers. The diblock polymers were synthesized from controlled ring-opening polymerization of L-lactide monomer using poly(ethylene glycol) methyl ether (M_n: 2K, 5K) as initiator and $SnOct_2$ as catalyst, which has been reported in detail elsewhere.[26] ^{1}H NMR ($CDCl_3$) δ (ppm) = 1.58 (−CO−CH(CH_3)−O−), 3.38 (CH_3−O−CH_2−), 3.45−3.48 (CH_3−O−CH_2−CH_2−), 3.65 (−O−CH_2−CH_2−O−), 5.14−5.23 (−CO−CH(CH_3)−O−).

Polymersome Fabrication. *Micron-Sized Polymersomes.* A thin-film hydration (TFH) method was utilized to fabricate PEG-*b*-(PLLA)$_2$ polymersomes in aqueous solutions. Briefly, a 10 mg polymer solution in 1 mL of chloroform was dried onto the walls of a 10 mL round-bottom flask at 60 °C under reduced pressure and kept under vacuum overnight; 1 mL of aqueous phosphate buffer (10 mM, pH 7.4) was subsequently added into the flask to hydrate the formed polymer film. After ultrasonication for 5 min in a bath sonicator (Aquasonic 75T), the solution was stirred continuously at 60 °C for 6 h.

Nano-Sized Polymersomes. (a) "Top-down" method: The above-prepared micrometer-sized polymersomes were subjected to ultrasonication up to 1 h at 60 °C using a Microson probe tip sonicator (output power 2 W, 23 kHz) and were subsequently extruded multiple times through a polycarbonate membrane (100 nm pore size) with an Avanti mini-extruder. (b) "Bottom-up" method: 100 μL of polymer solution in DMF (10 mg mL^{-1}) was injected into 1 mL phosphate buffer under vigorous stirring using a microsyringe. The resulting solution was stirred for half an hour and then transferred into a preswollen dialysis membrane (SPECTRA/POR; MWCO 10 000 Da) and dialyzed against aqueous buffer. The outer phase was replaced with fresh buffer solution at 1, 2, 4, 6, and 12 h. The solution inside the membrane was recovered after 24 h.

All of the above vesicle solutions were stirred for an additional 24 h at room temperature after preparation. All the following measurements were carried out at room temperature unless otherwise specified.

Gel Permeation Chromatography (GPC). GPC measurements were performed on an Agilent 1100 Series HPLC system equipped with a TSKgel G3000HHR GPC column and a refractive index detector using DMF with 10 mM LiBr as the eluent at 30 °C and calibrated with a series of PEG standards in the M_n range from ca. 300 to 40 000 Da. Representative GPC traces of the PEG-*b*-(PLLA)$_2$ polymers are shown in Figure S3.

Optical Microscopy (OM). OM observations were performed using the 40× objective lens on an Olympus CK X41 microscope that was equipped with a digital camera.

Confocal Laser Scanning Microscopy (CLSM). CLSM was performed on an Olympus FV-1000 confocal microscope. To prepare FITC-Dextran and Nile red loaded polymersomes by the TFH method, a 1 mg mL^{-1} FITC-Dextran aqueous solution with 10 mM phosphate buffer saline was applied to hydrate the polymer film, followed by 12 h of dialysis using a dialysis membrane (MWCO: 10 000 Da) to remove free FITC-Dextran molecules. Following dialysis, 2 μL of Nile red solution in DMF (1 mg mL^{-1}) was added to 2 mL of the FITC-Dextran loaded solution. After 1 day of equilibration at room temperature one drop of the suspension was placed on an adhesive microscope slide and viewed using the inverted CLSM equipped with an argon laser and a helium/neon mixed gas laser with excitation wavelengths of 488 and 543 nm, respectively. Clear differentiation between the fluorescence of the FITC and Nile red was achieved using optical band-pass filters of 505−530 nm and 605−660 nm in the channels of 488 and 543 nm, respectively. The single channel of 488 nm was employed to observe DOX-loaded polymersomes. Digital images of 1024 × 1024 pixels were recorded at a speed of 1.69 s/scan in the XY mode.

Dynamic Light Scattering (DLS) and Static Light Scattering (SLS). Light scattering experiments were carried out at angles from 30° to 120° using a Brookhaven Instruments Corp. system consisting of a BI-200SM goniometer and a BI-9000AT autocorrelator. The prepared polymersome solution was diluted to 0.1 mg mL^{-1} and was filtered using a 0.80 μm disposable membrane filter prior to measurement. The theories of DLS and SLS were described in the Supporting Information. Briefly, the field correlation function obtained from DLS was analyzed by the constrained regularized CONTIN method to yield the apparent translational diffusion coefficient D_{app} and the polydispersity index (PDI).[27,28]

The D_{app} is further correlated to the intrinsic diffusion coefficient D_0 via the following equation:

$$D_{app} = D_0(1+k_d c)(1+CR_g{}^2q^2) \quad (1)$$

where k_d is the effective interaction parameter, q the magnitude of the scattering wave vector, c the polymer concentration, R_g the radius of gyration, and C a parameter that is characteristic of the molecular architecture. Since $k_d c$ can be negligible for a very dilute solution, the intrinsic diffusion coefficient D_0 was obtained by extrapolating the experimental data of angular dependent diffusion coefficient (D_{app}) to zero angle.

The hydrodynamic radius (R_h) is related to D_0 via the Stokes−Einstein equation:

$$D_0 = kT/6\pi\eta R_h \quad (2)$$

where k is the Boltzmann constant and η is the viscosity of water at temperature T.

The z-average gyration of radius (R_g) was measured by static light scattering (SLS) via a simplified Rayleigh−Gans−Debye equation:[29]

$$\frac{1}{I_{ex}(\theta)} \approx k\left(1+\frac{\langle R_g{}^2\rangle}{3}q^2\right) \quad (3)$$

where k is an experimental constant and I_{ex} is the excess scattered intensity of the sample at the angle θ.

Critical Aggregation Concentration (CAC) Measurements. Incorporation of pyrene was achieved by injecting 2 μL of pyrene in ethanol stock solution into 3 mL of polymer solution with known concentrations (0.1−100 μg mL^{-1}), and the solution was stirred overnight. The final concentration of pyrene in the sample was 0.6 μM. The pyrene fluorescence excitation at λ_{em} = 393 nm was recorded for CMC determinations using a Shimadzu RF-5301PC spectrofluorometer. The fluorescence intensity ratios of two different bands (I_{336}/I_{333}) of pyrene were measured as a function of polymer concentration. An increase in this ratio was observed at a specific concentration, indicating the onset of polymer aggregation and thus the CAC. Representative plots of pyrene excitation spectra and variations in I_{336}/I_{333} as a function of the copolymer concentration for PEG$_{45}$-*b*-(PLLA$_{12.5}$)$_2$ are shown in Figure S4.

Transmission Electron Microscopy (TEM). TEM observations were performed on a Philips TECNAI T12 electron microscope. To prepare the sample, one drop of the aqueous

solution was deposited onto a Formvar-carbon-coated copper grid. 5 min later, excess solution was wicked away by touching the edge of the grid with a filter paper. The sample was then observed directly by TEM without staining.

Doxorubicin Encapsulation. Aqueous solution of ammonium sulfate (155 mM, pH 7.4) was used to prepare nano-sized polymersomes by the top-down method. The extruded samples were dialyzed against isoosmotic Dulbecco's phosphate buffered saline (DPBS, modified, without calcium chloride and magnesium chloride, pH = 7.4). Dialysis solutions were changed three times over ~12 h. The polymersomes were then incubated with DOX·HCl at a polymer/drug feed ratio of 1/0.2 (w/w) for 24 h at room temperature. Nonentrapped DOX was removed by dialysis against DPBS buffer for another 12 h. Subsequently, 10 μL of the DOX-loaded polymersome formulation was lyophilized, and the freeze-dried sample was redissolved in 1 mL of DMSO. The absorbance of the resulting solution was measured at 480 nm, and the drug concentration was determined from the standard curve which was created by measuring the absorbance of DOX·HCl solutions in DMSO with known concentrations (1−100 μg mL^{-1}) using a SPECTRAmax M2 UV−vis spectrophotometer. On the basis of the Lambert−Beer law, a linear regression equation relating the absorbance (A) to the DOX·HCl concentration (c, μg mL^{-1}) was obtained:

$$A = 0.025c, \quad r^2 = 0.996 \tag{4}$$

where r is the correlation coefficient.

***In Vitro* Drug Release Study.** The drug release experiments were carried out immediately after nonentrapped DOX was removed. 1.0 mL of DOX-loaded polymersome solution was added to the dialysis tubing and dialyzed against 50 mL of DPBS buffer at pH 7.4 in a 37 °C water bath under mechanic shaking (40 rpm). After predetermined time intervals, 5.0 mL of buffer was periodically extracted to determine the DOX concentration (c, μg mL^{-1}) at 480 nm by visible absorption spectrophotometry using the following calibration curve of DOX in the DPBS buffer.

$$A = 0.021c+0.004, \quad r^2 = 0.999 \tag{5}$$

The extracted volume was replaced by the addition of 5.0 mL of fresh buffer to maintain the sink condition.

Results

Polymer Synthesis and Characterizations. The PEG-based 3-miktoarm star copolymers were prepared by controlled ring-opening polymerization of L-lactide monomer using the synthesized hydroxyl-terminated dendron as macroinitiator (Scheme 2), and we denote them as PEG$_m$-*b*-(PLLA$_n$)$_2$ (the subscript indicates the degree of polymerization for each arm) while the PEG-*b*-PLLA diblock copolymers were prepared using a conventional ring-opening polymerization method.[26] Their molecular characteristics are listed in Table 1. It is noted that the volume fractions of PEG (f) ranged from 0.2 to 0.7 for the two series of polymers.

Micron-Sized Polymersome Formation. A thin-film hydration (TFH) method which is generally used for liposome preparation was utilized to fabricate self-assemblies of the PEG-*b*-(PLLA)$_2$ polymers in aqueous solutions (see the Experimental Section for details). In the resulting samples, spherical polymersomes with a diameter of ca. 1−3 μm were observed by optical microscopy (OM) (Figure 1a.1−1a.3). To further confirm the morphology of the formed self-assemblies, Nile red—a hydrophobic red dye—and FITC-Dextran (M_n ~ 4000 Da)—a hydrophilic green dye—were encapsulated into the hydrophobic bilayer and aqueous inner phase of the vesicles, respectively. After removing the free dyes, the membrane and the aqueous lumen were distinguishable from the distinct fluorescence of the encapsulated dyes using laser scanning confocal microscopy (LSCM) (Figure 1b.1−1b.3). Polymersome formation by the TFH method was confirmed for all of the 3-miktoarm polymers investigated in the f range of 0.2−0.7. In contrast, the linear PEG-*b*-PLLA copolymers with relatively low f values (0.21 and 0.37) formed micrometer-sized vesicles (Figure 2a), but for greater f values (0.57 and 0.70) only compound micelles (40−100 nm in diameter, Figure 2b) and individual spherical micelles (~20 nm in diameter, Figure 2c) were observed, respectively, by transmission electron microscopy (TEM), which is consistent with previous studies on diblock copolymers.[22−24] The summary of results shown in Table 1 thus reveals a superior capability to form polymersomes for the AB_2 type 3-miktoarm polymers compared to their diblock counterparts.

Nano-Sized Polymersome Formation. From a practical point of view, nano-sized polymersomes (typically 20−200 nm in diameter) are more promising as carriers for therapeutic agents, especially anticancer drugs, because these nanovehicles are able to passively accumulate in solid tumors due to the enhanced permeability and retention (EPR) effect.[30] Therefore, several attempts were made to fabricate nano-sized polymersomes using the PEG-*b*-(PLLA)$_2$ polymers. A "top-down" approach was applied in which the prepared microsized polymersomes were subject to further ultrasonication followed by multiple extrusions (refer to the Experimental Section). Consequently, nano-sized self-assemblies with a single diffusion mode and a relatively narrow size distribution (PDI = 0.10−0.15) were confirmed by dynamic light scattering (DLS) (Figure 3a). For PEG$_{45}$-*b*-(PLLA$_{32.5}$)$_2$, a value of 73 nm of the hydrodynamic radius (R_h) was obtained by extrapolating the apparent diffusion coefficient (D_{app}) to zero angle (Figure 3b). Static light scattering (SLS) measurements were performed to obtain the radius of gyration (R_g) based on the simplified Rayleigh−Gans−Debye equation (Figure 3c), and the R_g was determined as 74 nm. The ratio of R_g/R_h is known as a characteristic parameter of morphologies and microstructures for self-assemblies in solutions. The value of R_g/R_h (1.01) close to 1 suggests the presence of hollow spheres (vesicles) in the system.[31,32] The microstructure of the nanoparticles was further studied by TEM. The TEM micrographs clearly reveal a spherical morphology and bilayer structure for the polymersomes (Figure 4a), and their size range is consistent with the light scattering measurements. More TEM micrographs of the polymersomes prepared by this method are shown in Figure 4b,c, and a summary of the light scattering results is listed in Table 2.

It was found that nano-sized polymersomes could also be prepared by a "bottom-up" procedure, i.e., solvent precipitation method. In this approach, a small volume of polymer solution in dimethylformamide (DMF) was directly injected into the phosphate buffer under vigorous stirring. Since DMF is a common solvent for both the PEG and PLLA blocks whereas water is a selective solvent only for the PEG block, spontaneous self-assembly of the polymers occurred instantly following the injection as a result of the decreased solubility of PLLA in the aqueous buffer. After removing the organic solvent by dialysis, spherical nano-sized polymersomes were fabricated directly in this case as observed by TEM (Figure 4d). Moreover, it was found the polymersomes of PEG$_{45}$-*b*-(PLLA$_{32.5}$)$_2$ prepared by the above two methods are similar in size, and their size changed very little over a period of 20 days (Figure 5), which implies that the two

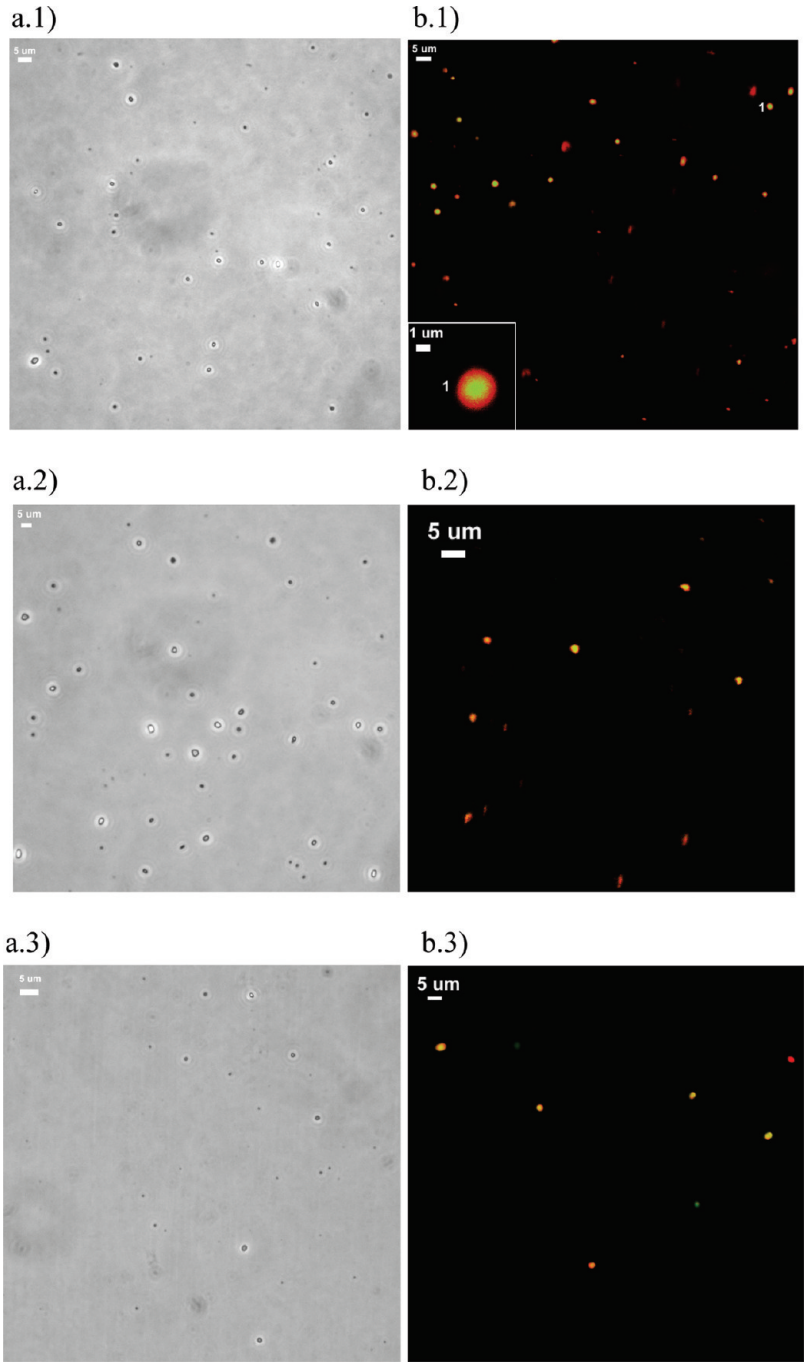

Figure 1. Polymersomes of (1) PEG_{45}-*b*-$(PLLA_{32.5})_2$ (f = 0.32), (2) PEG_{45}-*b*-$(PLLA_{12.5})_2$ (f = 0.55), and (3) PEG_{117}-*b*-$(PLLA_{17.5})_2$ (f = 0.70) observed by (a) OM and (b) LSCM (scale bars indicate 5 μm). The inset of (b.1) shows the magnified image of a Nile red/FITC-Dextran loaded polymersome as indicated by the number "1".

systems are probably in the same kinetically if not thermodynamically stable state.

Doxorubicin Encapsulation and *in Vitro* Drug Release. The hydrochloride salt of doxorubicin (DOX), namely DOX·HCl (Figure 6a), is a water-soluble anthracycline antibiotic widely used in cancer chemotherapy. In this study, DOX·HCl was used as a model drug to incorporate into the nano-sized polymersomes of PEG-*b*-$(PLLA)_2$ via a remoting loading method.[33] The mechanism of this method relies on creating an ammonium ion gradient across the vesicle membrane which allows DOX to actively accumulate inside the vesicle due to the huge difference in the permeability coefficient between neutral ammonia ($\sim$0.1 cm s^{-1}) and the SO_4^{2-} anion ($< 10^{-12}$ cm s^{-1}) as well as the efficient gelation of DOX sulfate in the intravesicular aqueous phase.[34] After removing the free drug, the loaded DOX inside the polymersomes was clearly visualized by LSCM imaging (Figure 6b). The drug loading efficiency was estimated to be 72 $\pm$ 5% for PEG_{45}-*b*-$(PLLA_{32.5})_2$ at a polymer concentration of 10 mg mL^{-1} and drug/polymer feed ratio of 0.2/1 (wt/wt).

The release profiles of the loaded DOX were studied *in vitro* over a period of 48 h and compared to free drug at the same equivalent concentration (Figure 7). For free DOX, the majority of the drug (ca. 90%) was quickly released within the first 5 h. In contrast, the release profile of the drug loaded inside the PEG_{45}-*b*-$(PLLA_{32.5})_2$ polymersomes showed two phases: in the first 2 h a small amount of drug leakage ($\sim$30%) took place, probably due to an initial burst release

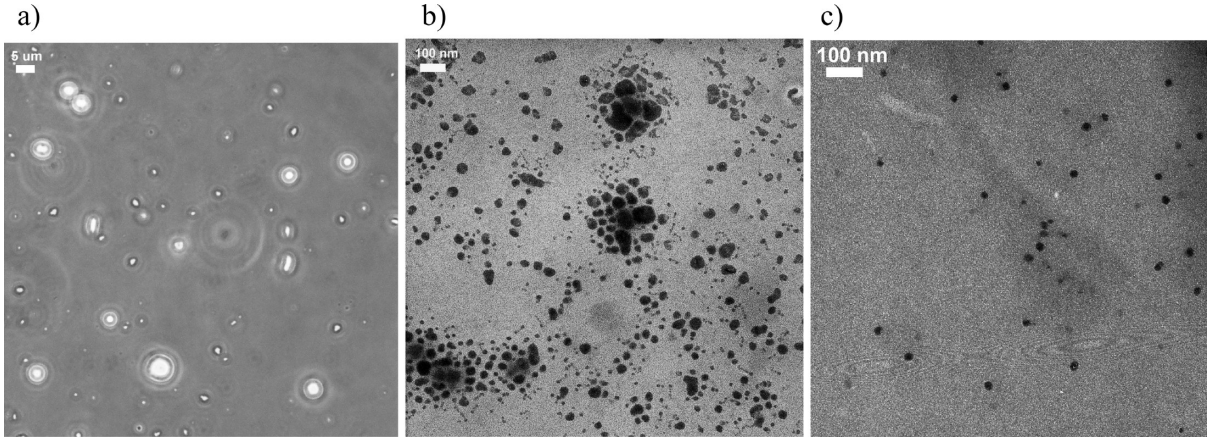

Figure 2. (a) OM micrograph of PEG_{45}-*b*-$PLLA_{53}$ polymersomes ($f = 0.37$). TEM micrographs of (b) PEG_{45}-*b*-$PLLA_{23}$ ($f = 0.57$) and (c) PEG_{117}-*b*-$PLLA_{34}$ ($f = 0.70$) micellar structures.

Table 1. Molecular Characterizations and Microstructures of the PEG-*b*-$(PLLA)_2$ and PEG-*b*-PLLA Polymers

sample ID	$M_{n(NMR)}$ ($\times 10^{-3}$ Da)	$M_{n(GPC)}$ ($\times 10^{-3}$ Da)	M_w/M_n [a]	f [b]	microstructure [c]
PEG-*b*-$(PLLA)_2$					
PEG_{45}-*b*-$(PLLA_{60.5})_2$	11.3	10.7	1.3	0.20	V
PEG_{45}-*b*-$(PLLA_{32.5})_2$	6.39	6.71	1.3	0.32	V
PEG_{117}-*b*-$(PLLA_{38})_2$	10.0	10.6	1.2	0.51	V
PEG_{45}-*b*-$(PLLA_{12.5})_2$	3.44	3.79	1.2	0.55	V
PEG_{117}-*b*-$(PLLA_{17.5})_2$	7.52	7.63	1.2	0.70	V
PEG-*b*-PLLA					
PEG_{45}-*b*-$PLLA_{115}$	10.4	10.3	1.2	0.21	V
PEG_{45}-*b*-$PLLA_{53}$	5.82	5.78	1.3	0.37	V
PEG_{45}-*b*-$PLLA_{23}$	3.55	3.68	1.1	0.57	SM, CM
PEG_{117}-*b*-$PLLA_{34}$	7.37	7.56	1.1	0.70	SM

[a] M_w/M_n was determined by GPC. [b] The volume fraction of PEG was calculated using M_n(GPC) and the densities of bulk polymers: ρ(PEG) = 1.13 g/cm^3, ρ(PLLA) = 1.25 g/cm^3. [c] V: vesicle; SM: spherical micelle; CM: compound micelle. The polymer self-assemblies were fabricated by the TFH method.

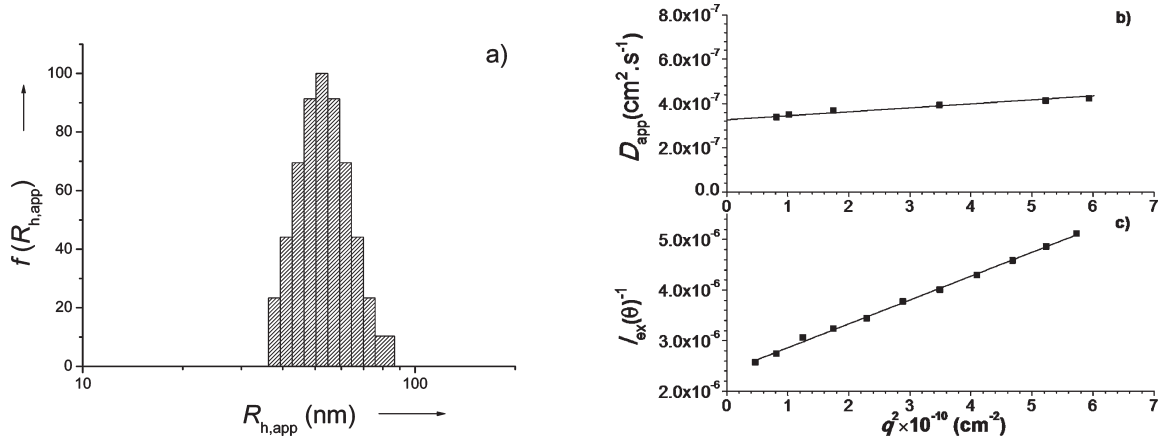

Figure 3. (a) Distribution of apparent hydrodynamic radius ($R_{h,app}$) at 90°. (b) Dependence of apparent diffusion coefficient (D_{app}) on the scattering wave vector (q) measured by DLS. (c) q dependence of excess scattered intensity $I_{ex}(\theta)$ obtained from SLS for the nano-sized polymersomes of PEG_{45}-*b*-$(PLLA_{32.5})_2$. Solid lines indicate the best linear fit.

of the drug located near the hydrophobic/hydrophilic interface of the vesicle membrane;[8] in the second stage, a remarkable sustained release was observed, and ca. 31% of the drug was still retained after 48 h. For the PEG_{45}-*b*-$(PLLA_{60.5})_2$ polymersomes, the loaded drug exhibited a release pattern similar to PEG_{45}-*b*-$(PLLA_{32.5})_2$, except for a lower initial burst release and more pronounced sustained release. Note that these two systems have the same length of A block (PEG) and similar vesicle size; therefore, the difference in the drug release profile should be attributed to the variation in the length of B block (PLLA). A longer hydrophobic block therefore tends to further enhance the drug retention effect of the polymersomes, which was also found in the linear diblock systems.[8] The *in vitro* drug release study thus suggested the potential application of these polymer vesicles as controlled drug delivery devices.

Critical Aggregation Concentrations. Critical aggregation concentration (CAC) is an important parameter to evaluate the themodynamic stability of a polymeric drug carrier under *in vitro*/*in vivo* conditions. The CAC values of the PEG-*b*-$(PLLA)_2$ and PEG-*b*-PLLA polymers were measured by a

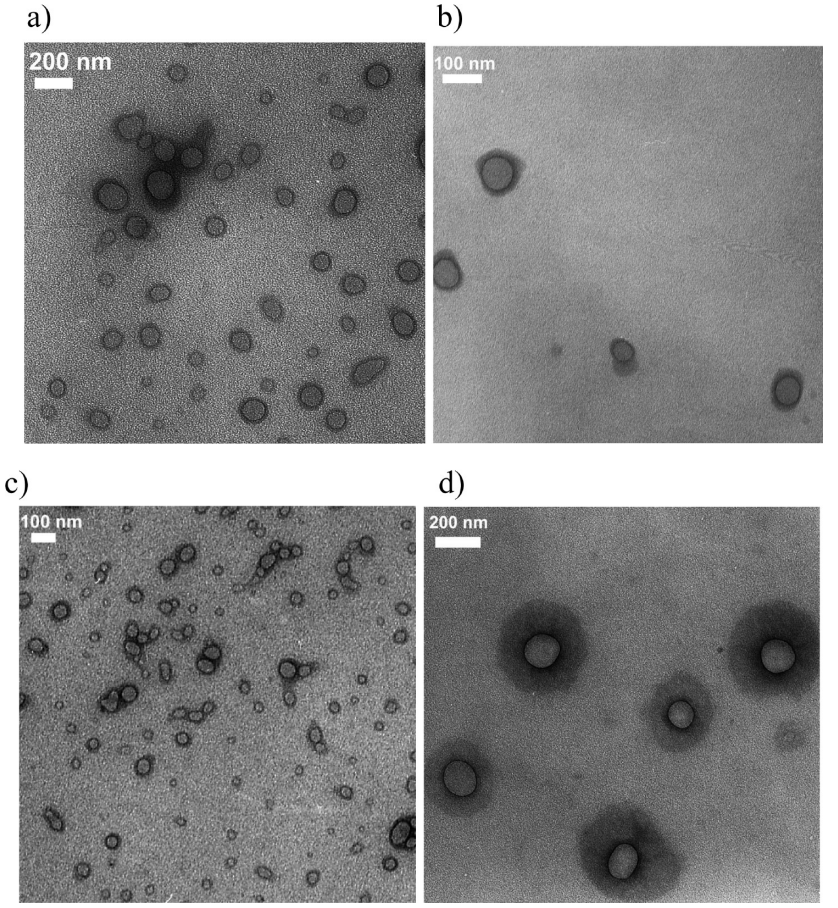

Figure 4. TEM micrographs of polymersomes of (a) PEG_{45}-*b*-$(PLLA_{32.5})_2$, (b) PEG_{45}-*b*-$(PLLA_{12.5})_2$, and (c) PEG_{117}-*b*-$(PLLA_{17.5})_2$ prepared by the top-down method. (d) TEM micrograph of PEG_{45}-*b*-$(PLLA_{32.5})_2$ polymersomes prepared by the bottom-up method.

Table 2. Light Scattering Characterizations of the Nano-Sized Polymersomes of the PEG-*b*-$(PLLA)_2$ Polymers

PEG-*b*-$(PLLA)_2$	R_g (nm)	R_h (nm)	R_g/R_h	PDI[a]
PEG_{45}-*b*-$(PLLA_{60.5})_2$	77	75	1.03	0.15
PEG_{45}-*b*-$(PLLA_{32.5})_2$	74	73	1.01	0.10
PEG_{117}-*b*-$(PLLA_{38})_2$	38	36	1.05	0.11
PEG_{117}-*b*-$(PLLA_{17.5})_2$	32	33	0.97	0.14

[a] Polydispersity index.

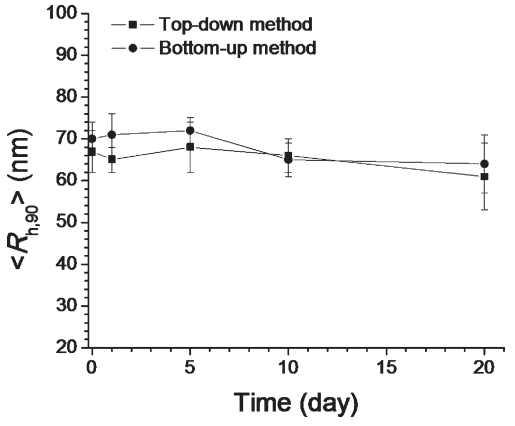

Figure 5. Time-dependent variations of the hydrodynamic radius at 90° ($\langle R_{h,90} \rangle$) for the PEG_{45}-*b*-$(PLLA_{32.5})_2$ polymersomes prepared by the top-down and bottom-up methods.

pyrene fluorescence probing method. From the results of Table 3, the PEG-*b*-$(PLLA)_2$ polymers had CAC values as low as several μg/mL. It is noteworthy that the CAC value of a PEG_m-*b*-$(PLLA_n)_2$ polymer is very close to that of its diblock counterpart, i.e., PEG_m-*b*-$PLLA_{2n}$ which has the same PEG block length and similar PLLA composition. The dependence of CAC on the length of PEG and PLLA blocks also followed the same trend for the two systems: an increase in the length of the PLLA block lead to a significant decrease in the CAC value whereas a variation in the PEG length had very little effect on it. The above results also suggest that the superior vesicle-forming capability of the AB_2 3-miktoarm star copolymers is probably closely related to their lipid-like structure.

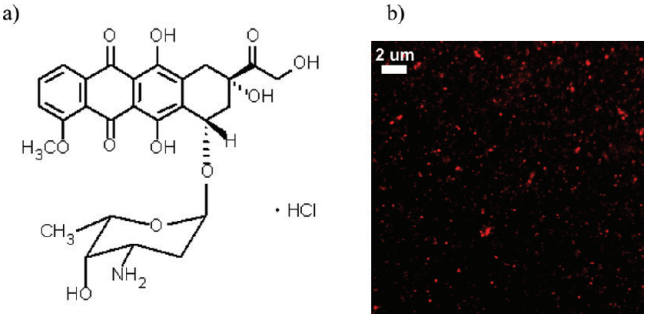

Figure 6. (a) Chemical structure of doxorubicin hydrochloride. (b) Fluorescence micrograph of DOX-loaded PEG_{45}-*b*-$(PLLA_{32.5})_2$ polymersomes observed by LSCM.

Discussion

This study demonstrated the superior vesicle-forming ability of AB_2 type 3-miktoarm star copolymers compared to their linear diblock counterparts. From the geometric point of view, the

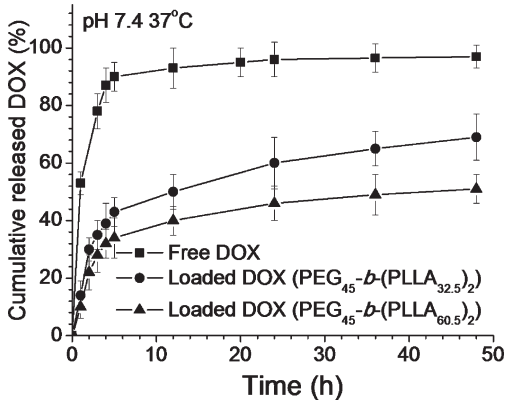

Figure 7. Cumulative DOX release profiles from loaded polymersomes compared with free drug at the same equivalent drug concentration (1 mg mL^{-1}) over a period of 48 h under *in vitro* conditions.

Table 3. Comparison of CAC Values between the PEG-*b*-(PLLA)$_2$ and PEG-*b*-PLLA Polymers

PEG-*b*-(PLLA)$_2$	CAC (μg/mL)	PEG-*b*-PLLA	CAC (μg/mL)
PEG_{45}-*b*-$(PLLA_{12.5})_2$	8.3 ± 1.5	PEG_{45}-*b*-$PLLA_{23}$	8.8 ± 0.8
PEG_{45}-*b*-$(PLLA_{32.5})_2$	1.1 ± 0.2	PEG_{45}-*b*-$PLLA_{53}$	1.3 ± 0.4
PEG_{45}-*b*-$(PLLA_{60.5})_2$	0.55 ± 0.15	PEG_{45}-*b*-$PLLA_{115}$	0.63 ± 0.11
PEG_{117}-*b*-$(PLLA_{17.5})_2$	8.9 ± 2.3	PEG_{117}-*b*-$PLLA_{34}$	9.1 ± 3.7

morphology of the self-assembled amphiphilic structures is primarily determined by the size of the hydrophobic moiety relative to the hydrophilic moiety. The theory of the critical packing parameter, *p*, proposed by Israelachvili et al.[35] has been widely used to explain the self-assembly formation of amphiphilic molecules in aqueous solutions (*p* is defined as v/al, where *v* is the hydrophobic volume of the amphiphile, *a* the interfacial area, and *l* the length of the hydrophobic part). Spherical micelles are formed on the condition that *p* is less than 1/3 while a value of *p* greater than 1/2 is required for vesicle formation. It can be expected that the *p* value of a A_m-*b*-$(B_n)_2$ polymer is markedly greater than its diblock counterpart A_m-*b*-$B_{(2n)}$ due to similar *a* and *v* values but a smaller *l* for the former one; therefore, vesicles are more likely to be formed at greater hydrophilic fractions for the AB_2 polymer. From the thermodynamic point of view, the aggregate morphologies are mainly governed by the interplay of three components of the free energy of aggregation, which include the stretching of the core-forming blocks, the interfacial free energy, and the intercorona interactions.[36] On the one hand, a micelle−vesicle transition normally takes place with an increase of *f* value for block copolymers due to an increasing spontaneous curvature.[37] On the other hand, both experimental and theoretical studies[38−40] on the microphase-separated AB_2 type bulk polymers have revealed that the Y-shape architecture can induce greater lateral crowding and chain stretching on the side of the B blocks compared to the linear diblock polymers, and the preferred curvature viewed from the B block side tends to decrease to alleviate the energetically unfavorable conformations. It is reasonable to consider there is a similar situation in an aqueous solution of amphiphilic AB_2 polymers which will push the system toward microstructures with less curvature. As a result, vesicular structures can still be thermodynamically favorable for the 3-miktoarm polymer at relatively higher *f* values whereas micelles are already the dominant aggregates for the linear counterpart. It should be mentioned that we did not try to obtain the exact upper/lower *f* value limits of the 3-miktoarm polymers for vesicle formation as they may vary for different systems depending upon a variety of physicochemical factors such as temperature, polymer−solvent interactions, and the presence of additives.

In fact, the above mechanisms are also supported by the experimental results of other research groups.[41−43] It was recently reported that vesicles can be formed for another AB_2 3-miktoarm copolymer (A = poly(methyl vinyl ether), B = polyisobutylene) with a hydrophilic fraction value as high as 0.85.[41] Zhou and Yan et al. found that hyperbranched star copolymers (PEO-*star*-HBPO) can self-assemble into giant vesicles in water even for an f_{PEG} value of 0.95,[42] which may be considered as one of the extreme instances. Hence, it is promising that the AB_2 architecture would provide a wider choice of hydrophilic/hydrophobic compositions for various polymer designs with vesicle-forming capabilities.

Conclusion

In conclusion, our study demonstrated that micrometer-/nano-sized vesicles can be fabricated from amphiphilic AB_2 type 3-miktoarm star copolymers in aqueous solutions. The lipid-like architecture showed superior vesicle-forming ability compared to the linear diblock structure. Thus, it may have some potential to become a versatile scaffold for various polymersome-based delivery systems. Future studies will investigate *in vitro* cytotoxicity of the DOX-loaded polymersomes against human tumor cells and biodegradability of the polymers. In the meantime, more novel 3-miktoarm polymers will be explored in attempts to develop functional polymersomes for smart drug delivery.

Acknowledgment. The first author is grateful to Nancy Chandler for help with the TEM observations and Deepa Mishra for her editorial aid.

Supporting Information Available: NMR plots of PEG_{45}-based dendron and NMR plot of PEG_{45}-*b*-$(PLLA_{32.5})_2$; GPC traces of PEG_{45}-*b*-$(PLLA_{32.5})_2$, PEG_{117}-*b*-$(PLLA_{38})_2$, and PEG_{45} and PEG_{117} polymers; pyrene excitation spectra and variations of I_{336}/I_{333} as a function of the copolymer concentration for PEG_{45}-*b*-$(PLLA_{12.5})_2$. This material is available free of charge via the Internet at http://pubs.acs.org.

References and Notes

(1) Andresen, T. L.; Jensen, S. S.; Jorgensen, K. *Prog. Lipid Res.* **2005**, *44* (1), 68–97.
(2) Gabizon, A. A.; Shmeeda, H.; Zalipsky, S. *J. Liposome Res.* **2006**, *16* (3), 175–183.
(3) Sackmann, E. Physical basis of self- organization and function of membranes: physics of vesicles. In *Structure and Dynamics of Membranes - From Cells to Vesicles*; Lipowsky, R., Sackmann, E., Eds.; Elsevier Science: Amsterdam, 1995.
(4) Discher, D. E.; Eisenberg, A. *Science* **2002**, *297* (5583), 967–973.
(5) Discher, B. M.; Won, Y. Y.; Ege, D. S.; Lee, J. C.; Bates, F. S.; Discher, D. E.; Hammer, D. A. *Science* **1999**, *284* (5417), 1143–1146.
(6) Discher, D. E.; Ahmed, F. *Annu. Rev. Biomed. Eng.* **2006**, *8*, 323–41.
(7) Antonietti, M.; Forster, S. *Adv. Mater.* **2003**, *15* (16), 1323–1333.
(8) Zhou, W.; Feijen, J. *J. Controlled Release* **2008**, *132*, e35–e36.
(9) Letchford, K.; Burt, H. *Eur. J. Pharm. Biopharm.* **2007**, *65* (3), 259–69.
(10) Burke, S.; Eisenberg, A. *High Perform. Polym.* **2000**, *12* (4), 535–542.
(11) Lee, J. C. M.; Bermudez, H.; Discher, B. M.; Sheehan, M. A.; Won, Y. Y.; Bates, F. S.; Discher, D. E. *Biotechnol. Bioeng.* **2001**, *73* (2), 135–145.
(12) Ghoroghchian, P. P.; Li, G. Z.; Levine, D. H.; Davis, K. P.; Bates, F. S.; Hammer, D. A.; Therien, M. J. *Macromolecules* **2006**, *39* (5), 1673–1675.
(13) Meng, F. H.; Hiemstra, C.; Engbers, G. H. M.; Feijen, J. *Macromolecules* **2003**, *36* (9), 3004–3006.
(14) Arifin, D. R.; Palmer, A. F. *Biomacromolecules* **2005**, *6* (4), 2172–81.
(15) Li, S.; Byrne, B.; Welsh, J.; Palmer, A. F. *Biotechnol. Prog.* **2007**, *23* (1), 278–85.

(16) Cerritelli, S.; Velluto, D.; Hubbell, J. A. *Biomacromolecules* **2007**, *8* (6), 1966–72.
(17) Borchert, U.; Lipprandt, U.; Bilang, M.; Kimpfler, A.; Rank, A.; Peschka-Suss, R.; Schubert, R.; Lindner, P.; Forster, S. *Langmuir* **2006**, *22* (13), 5843–5847.
(18) Meng, F.; Engbers, G. H.; Feijen, J. *J. Controlled Release* **2005**, *101* (1−3), 187–98.
(19) Lomas, H.; Canton, I.; MacNeil, S.; Du, J.; Armes, S. P.; Ryan, A. J.; Lewis, A. L.; Battaglia, G. *Adv. Mater.* **2007**, *19* (23), 4238–4243.
(20) Ahmed, F.; Pakunlu, R. I.; Brannan, A.; Bates, F.; Minko, T.; Discher, D. E. *J. Controlled Release* **2006**, *116* (2), 150–158.
(21) Christian, D. A.; Cai, S.; Bowen, D. M.; Kim, Y.; Pajerowski, J. D.; Discher, D. E. *Eur. J. Pharm. Biopharm.* **2009**, *71* (3), 463–74.
(22) Discher, D. E.; Ortiz, V.; Srinivas, G.; Klein, M. L.; Kim, Y.; Christiana, D.; Cai, S.; Photos, P.; Ahmed, F. *Prog. Polym. Sci.* **2007**, *32*, 838–857.
(23) Srinivas, G.; Discher, D. E.; Klein, M. L. *Nat. Mater.* **2004**, *3* (9), 638–644.
(24) Won, Y. Y.; Brannan, A. K.; Davis, H. T.; Bates, F. S. *J. Phys. Chem. B* **2002**, *106* (13), 3354–3364.
(25) Zhang, L. F.; Eisenberg, A. *Polym. Adv. Technol.* **1998**, *9* (10−11), 677–699.
(26) Liggins, R. T.; Burt, H. M. *Adv. Drug Delivery Rev.* **2002**, *54* (2), 191–202.
(27) Chu, B. *Laser Light Scattering*; Academic Press: New York, 1990.
(28) Provencher, S. W. *Biophys. J.* **1976**, *16*, 27–41.
(29) Kistler, M. L.; Bhatt, A.; Liu, G.; Casa, D.; Liu, T. *J. Am. Chem. Soc.* **2007**, *129* (20), 6453–60.
(30) Maeda, H.; Wu, J.; Sawa, T.; Matsumura, Y.; Hori, K. *J. Controlled Release* **2000**, *65* (1−2), 271–84.
(31) Zhou, S. Q.; Burger, C.; Chu, B.; Sawamura, M.; Nagahama, N.; Toganoh, M.; Hackler, U. E.; Isobe, H.; Nakamura, E. *Science* **2001**, *291* (5510), 1944–1947.
(32) Liu, T. B.; Diemann, E.; Li, H. L.; Dress, A. W. M.; Muller, A. *Nature* **2003**, *426* (6962), 59–62.
(33) Haran, G.; Cohen, R.; Bar, L. K.; Barenholz, Y. *Biochim. Biophys. Acta* **1993**, *1151* (2), 201–15.
(34) Barenholz, Y. *Curr. Opin. Colloid Interface Sci.* **2001**, *6*, 66–77.
(35) Israelachvili, J. N.; Mitchell, D. J.; Ninham, B. W. *J. Chem. Soc., Faraday Trans. 2* **1976**, *72*, 1525–1568.
(36) Flory, P. J. *Principles of Polymer Chemistry*; Cornell University Press: Ithaca, NY, 1971.
(37) Soo, P. L.; Eisenberg, A. *J. Polym. Sci., Part B: Polym. Phys.* **2004**, *42* (6), 923–938.
(38) Pochan, D. J.; Gido, S. P.; Pispas, S.; Mays, J. W.; Ryan, A. J.; Fairclough, J. P. A.; Hamley, I. W.; Terrill, N. J. *Macromolecules* **1996**, *29*, 5091–5098.
(39) Lee, C.; Gido, S. P.; Pitsikalis, M.; Mays, J. W.; Tan, N. B.; Trevino, S. F.; Hadjichristidis, N. *Macromolecules* **1997**, *30*, 3732–3738.
(40) Milner, S. T. *Macromolecules* **1994**, *27*, 2333–2335.
(41) Yun, J. P.; Faust, R.; Szilagyi, L. S.; Keki, S.; Zsuga, M. *Macromolecules* **2003**, *36* (5), 1717–1723.
(42) Zhou, Y.; Yan, D. *Angew. Chem., Int. Ed.* **2004**, *43* (37), 4896–9.
(43) Zhou, Y.; Yan, D.; Dong, W.; Tian, Y. *J. Phys. Chem. B* **2007**, *111* (6), 1262–70.